ENERGY DISSIPATION IN PARTIALLY PRESTRESSED CONCRETE BEAMS UNDER REVERSED CYCLIC LOADING AND DAMAGE EVALUATION

(Translation from Journal of Materials, Concrete Structures and Pavements, No.496/V-24, August 1994)

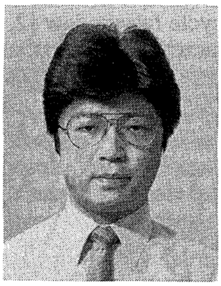
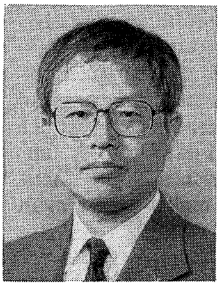
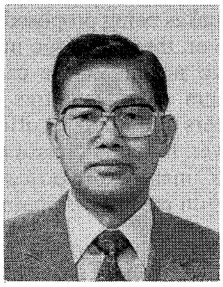

Susumu INOUE　　Toyoaki MIYAGAWA　　Manabu FUJII

We investigate the effects of mechanical degree of prestress, volumetric ratio of lateral confinement, concrete compressive strength, steel index, and shear span effective depth ratio on the energy dissipation properties of partially prestressed concrete beams under different loading histories. The relationships between these test variables and non-dimensional dissipated energy are derived based on the test results. Results indicate that seismic damage to partially prestressed concrete beams can be evaluated quantitatively using a proposed damage index based on hysteretic dissipated energy.

Keywords: *partially prestressed concrete, non-dimensional dissipated energy, loading history, mechanical degree of prestress, volumetric ratio of lateral confinement, damage evaluation*

Susumu Inoue is Associate Professor of Civil Engineering at Osaka Institute of Technology, Osaka, Japan. He received his Doctor of Engineering Degree from Kyoto University in 1994. His research interests include the ductility improvement of reinforced and prestressed concrete members and seismic damage evaluation of concrete structures. He is a member of the JSCE, JCI, and JSMS.

Toyoaki Miyagawa is Associate Professor of Civil Engineering at Kyoto University, Kyoto, Japan. He received his Doctor of Engineering Degree from Kyoto University in 1985. He is the author of a number of papers dealing with the durability of reinforced concrete structures. He is a member of the JSCE, ACI, JSMS, and a number of technical committees.

Manabu Fujii is Professor of Civil Engineering at Kyoto University, Kyoto, Japan. He received his Doctor of Engineering Degree from Kyoto University in 1972. His current research activities are focused on the optimal design of prestressed concrete cable-stayed bridges, structural safety evaluations, and the durability of concrete structures. He has written some 50 papers on these subjects. He is a member of the JSCE, ACI, JCI, JSMS, and a number of technical committees.

1. INTRODUCTION

It is very important to be able evaluate seismic damage to concrete structures quantitatively and precisely in order to judge the serviceability of such structures after an earthquake, and the need for repair and/or strengthening. In general, seismic damage is judged mainly by a site inspection of the damaged structures. Based on the results of such inspections, the residual deformability of the damaged structures is evaluated along with the maximum response deformation [1]. The safety of concrete structures under seismic loading is usually estimated from the deformation ductility, so it is important to relate the degree of damage to the residual deformability.

It is also well known that the ductility of concrete members under reversed cyclic loading such as experienced during an earthquake is significantly lower than that under monotonous loading. This implies that seismic damage to concrete structures and members should be evaluated by taking into consideration damage accumulation due to cyclic load reversals and repetitions.

This situation has led to certain damage indexes that take into account the damage accumulation during earthquakes being proposed based on hysteretic energy dissipation or low–cycle fatigue law [2, 3, 4]. However, these damage indexes are based on test results for reinforced concrete (RC) members and they do not cover the case of partially prestressed concrete (PPC) or prestressed concrete (PC) members. PPC structures have attracted attention recently for the high degree of freedom they give designers and they are often used for members subjected to earthquake loading as structural beams. However, the energy dissipation properties of PPC members are affected by many factors as compared with RC members. Consequently, it is necessary to quantitatively clarify the effects of these various factors on energy dissipation in order to make precise evaluation of damage during earthquakes.

In this paper, the effects of various factors on the accumulation of dissipated energy in PPC beams – which ultimately fail in flexure under reversed cyclic loading – are discussed based on results obtained in experiments done by the authors [5~10]. In addition, a new damage index based on the total energy dissipated up to the ultimate state is proposed.

2. EXPERIMENTAL PROCEDURE

2.1 Test Variables

A large number of factors have an influence on the energy dissipation properties of PPC beams. In this paper, however, the following five test variables, which are expected to have a relatively large influence, are selected:

a) Volumetric ratio of lateral confinement (ρ_s)

The volumetric ratio of lateral confinement ρ_s is defined by the equation

$$\rho_s = \frac{\textbf{volume of one transeverse hoop}}{\textbf{volume of core concrete confined by one hoop}} \times 100\ (\%) \tag{1}$$

b) Mechanical degree of prestress (λ)

The mechanical degree of prestress λ is defined as

$$\lambda = \frac{A_p f_{py}}{A_p f_{py} + A_s f_{sy}} \tag{2}$$

Where,

A_p: area of prestressing steel
f_{py}: yield strength of prestressing steel
A_s: area of non–tensioned deformed bar
f_{sy}: yield strength of non–tensioned deformed bar

c) Concrete compressive strength (f'_c)

d) Steel index (q)

The steel index q is defined as Equation (3).

$$q=q_p+q_s=\frac{A_p f_{py}}{bd_p f'_c}+\frac{A_s f_{sy}}{bd_s f'_c} \quad (3)$$

Where,
b: width of cross section
d_p: effective depth of prestressing steel
d_s: effective depth of non-tensioned deformed bar
f'_c: compressive strength of concrete

e) Shear span – effective depth ratio (a/d)

Table 1 Details of Test Variables

	Series-A	Series-B	Series-C	Series-D
ρ_s (%)	0, 0.6, 1.2, 2.4	0.6, 1.2, 2.4	0.6, 1.2, 2.4	0, 0.6, 1.2, 2.4
λ	0.4, 0.7, 1.0	0.4, 0.7, 1.0	0.4, 0.7, 1.0	0.4, 0.7, 1.0
f'_c (MPa)	40, 80	40	40	40, 80
σ_{cp} (MPa) *	5, 8, 10, 12, 23	5, 8, 12	5, 8, 12	5, 8, 10, 12, 23
q	0.2, 0.25, 0.3,	0.25, 0.3	0.25, 0.3	0.2, 0.25, 0.3
a/d	2.3, 2.9, 3.5	2.3, 2.9, 3.5	3.5	3.5
number of specimens	63	19	9	24

* σ_{cp}: introduced prestress

Details of the adopted values of these test variables are listed in Table 1 for each series of loading tests. In all test specimens, the tensile stress in the prestressing bars immediately after prestressing was adjusted to be 70% of their tensile strength. Accordingly, the introduced effective prestress in concrete is approximately 5MPa, 8MPa, and 12MPa for λ =0.4, 0.7 and 1.0, respectively, in the case of f'_c =40MPa. On the other hand, the introduced prestress in specimens with f'_c=80MPa is 10MPa and 23MPa for λ =0.4 and 1.0, respectively.

2.2 Specimens

Specimens used for the loading tests were simple beams of partially prestressed concrete, including also fully prestressed concrete beams, with a rectangular cross section of b x h = 10 x 20cm (b:width, h:full depth of section) and a total length of 160cm. As shown in Fig.1, they were symmetrically reinforced with prestressing bars and non-prestressing deformed bars. The effective depth of the lower prestressing bar (d_p) is 15cm for all the beams. SD295A deformed mild bars (f_{sy} ≒ 350N/mm^2) are used for longitudinal non-tensioned bars, except in the λ =1.0 beams, in which ϕ 6mm round bars (f_{sy}=495N/mm^2) were used to fabricate the steel cage. In this case, the real value of λ is slightly smaller than 1.0 considering the longitudinal reinforcing effect of these ϕ 6mm bars. As lateral confinement and shear reinforcement, ϕ 6mm rectangular closed hoops with 135° hooks at the corners (f_{sy}=495N/mm^2) were used. The spacing of the shear reinforcement was chosen in accordance with the JSCE's Standard Specification for Design and Construction of Reinforced Concrete Structures in order to prevent premature shear failure. As prestressing steel, round prestressing bars (SBPR A-1, B-1 and C-1) were used in all specimens. These prestressing

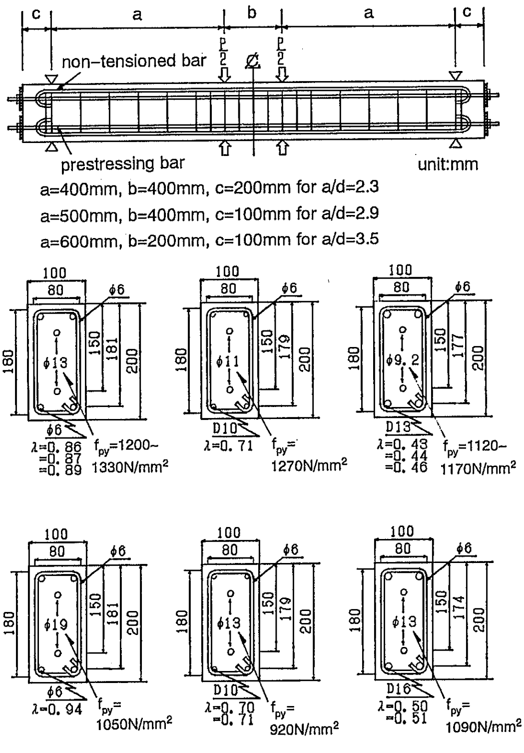

Fig.1 Dimensions of Specimens

bars were post–tensioned and grouted with cement paste of W/C=45%.

2.3 Loading Histories

In this paper, the following four loading histories are adopted in order to investigate the effects of loading history on energy dissipation properties.

a) Series–A

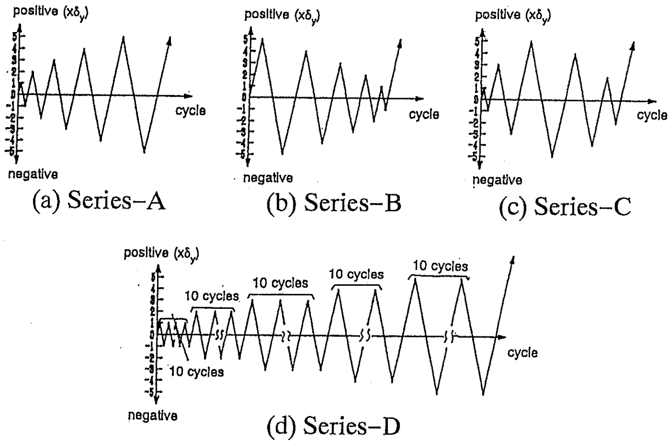

Fig.2 Applied Loading Histories

Series–A consists of gradually increasing reversed cyclic loading with one load reversal at each deflection amplitude. In this series, the applied deflection amplitude is gradually increased, e.g. 1 δ_y (δ_y: yield deflection), 2 δ_y, 3 δ_y, ... up to the deflection amplitude, where the load carrying capacity is reduced to 80% of the maximum load (δ_u). The yield deflection δ_y is obtained from the measured load–deflection curve and is somewhat larger than the calculated value (δ_{ycal}) derived by using the actual yield strength of the reinforcing bars and prestressing bars. This implies that both reinforcing bars and prestressing bars have already yielded at δ_y.

b) Series–B

Series–B consists of gradually decreasing reversed cyclic loading with one load reversal at each deflection amplitude, in which the applied deflection amplitude is gradually decreased from δ_u to δ_y. The sum of the applied deflection amplitudes is adjusted to equal that of Series–A.

c) Series–C

Series–C consists of mixed Series–A and Series–B loading, in which the applied deflection amplitude is first gradually increased up to δ_u and then gradually decreased. The sum of the applied deflection amplitudes in Series–C is also equal to that of Series–A.

d) Series–D

Series–D is gradually increasing reversed cyclic loading with ten load reversals at each deflection amplitude.

These loading histories are shown schematically in Fig.2. Specimens were tested under symmetrical two–point loading with various shear span lengths and flexural span lengths corresponding to the a/d ratio. After the prescribed loading sequences, all specimens were subjected to additional loading cycles until their load carrying capacity fell to approximately 50% of the maximum.

3. RESULTS OF TESTS AND DISCUSSIONS

3.1 Definition of the Ultimate State and Non–dimensional Dissipated Energy

It is necessary to define the ultimate state of members if seismic damage to concrete structures is to be evaluated. In this paper, the ultimate state is defined as the point at which the load carrying capacity has fallen to 80% of the maximum load. All tested specimens reached their ultimate state as a result of crushing and spalling of concrete within the flexural span as more cycles were applied after yielding of the tensile reinforcement.

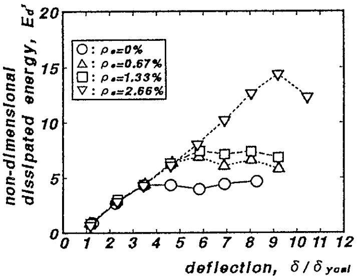

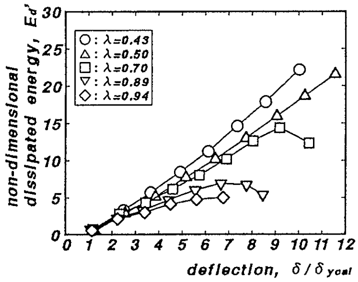

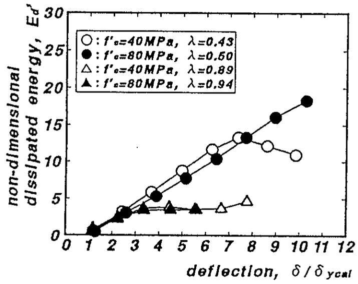

Fig.3 Effects of ρ_s on E_d' Value (Series–A, λ =0.70)

Fig.4 Effects of λ on E_d' Value (Series–A, ρ_s≒2.50%)

Fig.5 Effects of f'_c on E_d' Value (Series–A, ρ_s≒1.25%)

On the other hand, the dissipated energy at each deflection amplitude (E_d) is equal to the area surrounded by each loop in the load–deflection hysteresis. Dissipated energy itself, however, varies greatly under different loading conditions for the same section. Therefore, non–dimensional dissipated energy at each deflection amplitude (E_d') is defined in this paper as follows,

$$E_d' = \frac{E_d}{P_{ycal}\,\delta_{ycal}} \tag{4}$$

where, P_{ycal} and δ_{ycal} are the calculated yield load and yield deflection of each beam, respectively. This eliminates the effect of differences in maximum load carrying capacity among the beams.

3.2 Effects of Test Variables on Energy Dissipation

a) Effects of volumetric ratio of lateral confinement (ρ_s)

Figure 3 shows the effects of volumetric ratio of transverse hoops (ρ_s) on the energy dissipation of Series–A beams; the horizontal axis represents non–dimensional applied deflection amplitude (δ / δ_{ycal}) and the vertical axis is the non–dimensional dissipated energy (E_d') at each deflection amplitude.

As Fig.3, the E_d' value increases almost linearly with increasing deflection amplitude within the range of relatively small applied deformation and the rate of increase is almost constant irrespective of ρ_s value given that the other test variables are the same. The E_d' value of a beam with a smaller ρ_s value, however, stops increasing or begins to decrease at smaller deflection amplitudes. This is because the beams with a smaller ρ_s value exhibit significant strength degradation at smaller deflection amplitudes, resulting in reduced energy dissipation later. In other words, the point after which the E_d' value does not increase linearly can be correlated with a point of significant strength reduction – that is, the ultimate state of the beam.

b) Effects of mechanical degree of prestress (λ)

Figure 4 shows the effects of mechanical degree of prestress (λ) on E_d' values for beams with ρ_s of approximately 2.5%. As seen in this figure, for the particular deflection amplitude, the E_d' value becomes smaller with increasing λ. This is because the area enclosed by each hysteresis loop becomes smaller with increasing λ.

c) Effects of concrete compressive strength (f'_c)

Figure 5 shows the E_d' values of the beams made with concrete of different compressive strengths. The E_d value of the f'_c=40MPa beam is somewhat larger than that of the f'_c=80MPa beam at the same

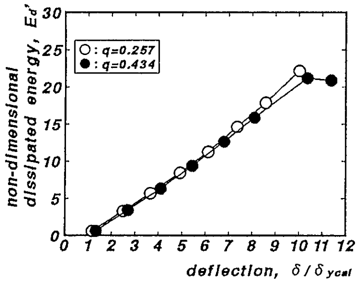

Fig.6 Effects of q on E_d' Value
(Series–A, $\lambda \fallingdotseq 0.45$, $\rho_s \fallingdotseq 2.50\%$)

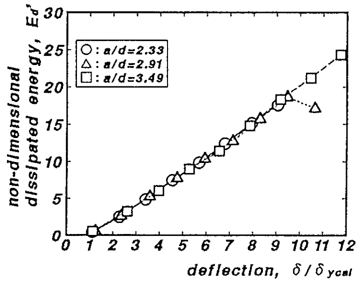

Fig.7 Effects of a/d on E_d' Value
(Series–A, λ =0.46, ρ_s=2.43%)

deflection amplitude. However, the λ value of the former is 0.43 (0.89) and somewhat smaller than that of the latter, which is 0.50 (0.94). Therefore, considering the difference in λ value between these two beams, the effect of concrete compressive strength can be seen to be smaller than that of volumetric ratio of lateral confinement and mechanical degree of prestress.

d) Effects of steel index (q)

Figure 6 shows an example of E_d' values of beams with different steel indexes; that is, q=0.257 and 0.434. The figure indicates that the E_d' values of these two beams at the same deflection amplitude are almost equal. Therefore, the effects of steel index on the non–dimensional dissipated energy can be considered to be negligible if the other test variables are the same.

e) Effects of shear span–effective depth ratio (a/d)

In Fig.7, E_d' values of beams loaded under different a/d ratios are shown. The E_d' value at a particular non–dimensional deflection amplitude is almost the same irrespective of the a/d ratio. With different a/d ratios, the acting shear force differs even if the applied deflection amplitude is the same. In these tests, however, each specimen was reinforced according to the maximum shear force, so energy dissipation properties were almost identical since flexure is more predominant than shear. This result implies that the effects of a/d ratio on non–dimensional dissipated energy are small if a beam is designed to fail in flexure even when loaded under a smaller a/d ratio within the range of 2.33~3.77 adopted in these tests.

3.3 Energy Dissipation Properties under Different Loading Histories

From the results of the Series–A tests, it is clear that the effects of concrete compressive strength, steel index, and shear span–effective depth ratio on the accumulation of non–dimensional dissipated energy are relatively small as compared with volumetric ratio of lateral confinement and mechanical degree of prestress. Here, then, the process of non–dimensional dissipated energy accumulation up to the ultimate state under different loading histories is discussed mainly in the light of the effects of mechanical degree of prestress and volumetric ratio of lateral confinement.

a) Series–A

In Fig.8 are shown the relationships between non–dimensional dissipated energy (E_d') and normalized applied deflection amplitude (δ / δ_{ycal}) for the Series–A beams. The E_d' value of each Series–A beam increases almost linearly with increasing applied deflection amplitude up to the ultimate state. As previously shown in Fig.3, the volumetric ratio of lateral confinement affects only the deflection amplitude at the point where the E_d' value stops increasing linearly, that is, at ultimate deflection. On the other hand, the gradient of the initial linear section is affected by the mechanical degree of prestress, made clear by Fig.4. Considering these results, the relationship between E_d' and δ / δ_{ycal} can be expressed in linear form as follows.

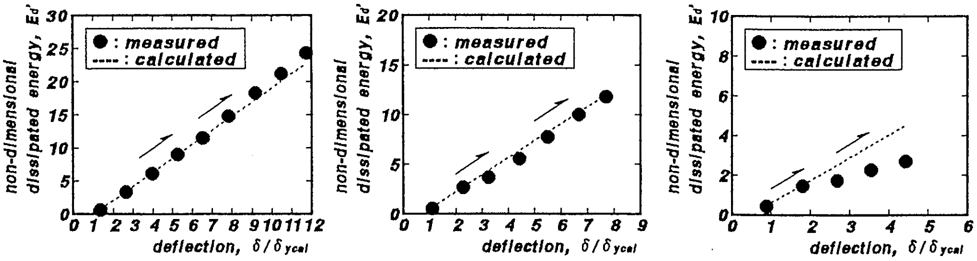

(a) λ =0.46 (b) λ =0.71 (c) λ =0.87

Fig.8 Examples of Relationships between E_d' and δ/δ_{ycal} (Series–A, ρ_s=2.43%)

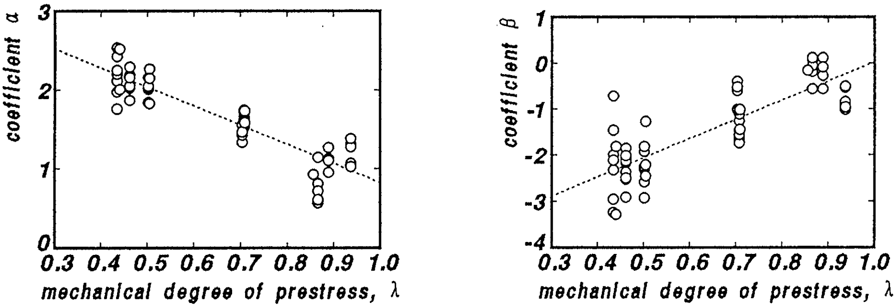

(a) coefficient α (b) coefficient β

Fig.9 Relationships between Coefficients α, β, and λ

$$E_d' = \alpha \frac{\delta}{\delta_{ycal}} + \beta \qquad (\delta \geqq \delta_{ycal}) \tag{5}$$

Where, α and β are functions of the mechanical degree of prestress λ.

The relationships between the coefficients α, β, and λ are shown in Figs.9–(a) and (b), respectively. The coefficients α and β in Eq.(5) are assumed to be linear functions of λ, although some scatter is observed. They can be expressed as in Eq.(6) and Eq.(7) from a regression analysis of the test data.

$$\alpha=-2.43\,\lambda+3.25 \qquad (0.43 \leqq \lambda \leqq 0.94) \tag{6}$$

$$\beta=4.17\,\lambda-4.15 \qquad (0.43 \leqq \lambda \leqq 0.94) \tag{7}$$

Figure 8 also shows calculated E_d' values derived from the regression analysis mentioned above. As indicated in Fig.8, the calculated values derived from Eq.(5)~Eq.(7) coincide well with the measured values. In some beams with larger λ values, however, the difference between measured and calculated E_d' values tends to be greater in the larger deflection amplitude range near the ultimate state due to the instability of the dissipated energy.

b) Series–B

Figure 10 shows some examples of the relationships between E_d' and δ/δ_{ycal} for the Series–B beams.

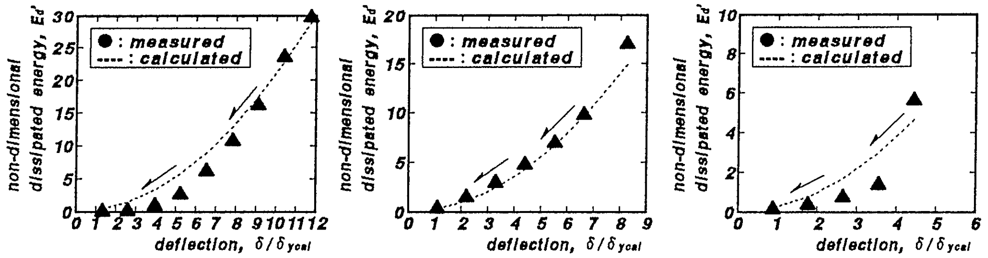

(a) λ =0.46 (b) λ =0.71 (c) λ =0.87

Fig.10 Examples of Relationships between E_d' and δ/δ_{ycal} (Series–B, ρ_s=2.43%)

In Series–B, the E_d' value is found to decrease almost quadratically when the applied deflection amplitude is gradually decreased from δ_u. This is because no new cracks occur for deflection amplitudes smaller than δ_u when deflection amplitude is gradually decreased, so there is less dissipated energy than in corresponding Series–A beams at the same deflection amplitude. Therefore, the relationship between E_d' and δ/δ_{ycal} can be written as Eq.(8).

$$E_d' = \gamma\left(\frac{\delta}{\delta_{ycal}}\right)^2 \quad (\delta \geqq \delta_{ycal}) \qquad \textbf{(8)}$$

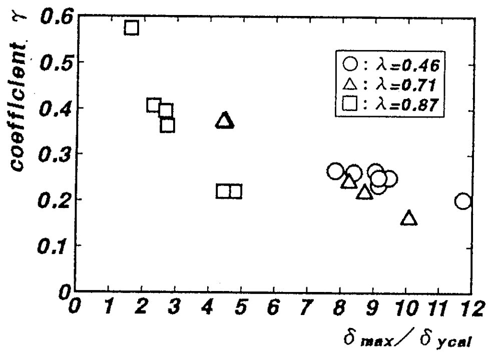

Fig.11 Relationship between Coefficient γ and $\delta_{max}/\delta_{ycal}$

The value of the coefficient γ is affected by the λ value and the maximum deflection amplitude in the first cycle (δ_{max}). Figure 11 shows the relationship between coefficient γ and $\delta_{max}/\delta_{ycal}$. As indicated in this figure, the γ value decreases almost in inverse proportion to $\delta_{max}/\delta_{ycal}$. As for the beams tested, the equations below are obtained from regression analysis of the experimental data.

$$\gamma = 1.494\left(\frac{\delta_{ycal}}{\delta_{max}}\right) + 0.083 \quad (\lambda=0.46) \qquad \textbf{(9)}$$

$$\gamma = 1.488\left(\frac{\delta_{ycal}}{\delta_{max}}\right) + 0.038 \quad (\lambda=0.71) \qquad \textbf{(10)}$$

$$\gamma = 0.879\left(\frac{\delta_{ycal}}{\delta_{max}}\right) + 0.036 \quad (\lambda=0.87) \qquad \textbf{(11)}$$

Figure 10 also shows calculated E_d' values at each deflection amplitude derived from Eq.(8)~Eq.(11). The calculated E_d' values coincide well with the measurements, although the agreement between the two for beams with λ =0.87 is not as good as that for λ =0.46 and 0.71. This is mainly because the relative reduction in E_d' value from the first cycle to the second tends to become larger with increasing λ value, while a quadratic reduction rate is assumed in the calculation irrespective of λ values.

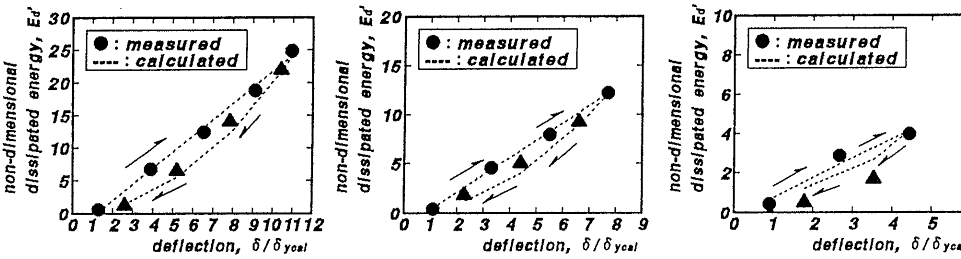

(a) λ =0.46 (b) λ =0.71 (c) λ =0.87

Fig.12 Examples of Relationships between E_d' and δ / δ_{ycal} (Series–C, ρ_s=2.43%)

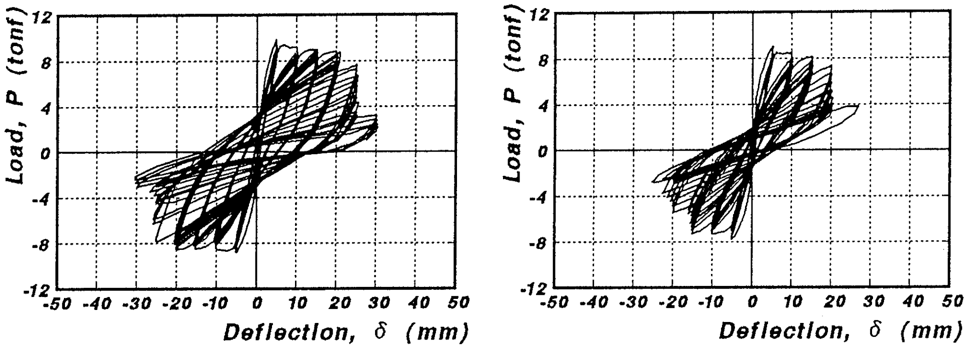

(a) λ =0.70 (b) λ =0.89

Fig.13 Examples of Load–Deflection Hysteresis Loops (Sereis–D, $\rho_s \fallingdotseq$2.50%)

c) Series–C

Figure 12 shows E_d'– δ / δ_{ycal} relationships for the Series–C beams. The behavior is almost the same as that seen in Series–A beams as the deflection is increased. On the other hand, the behavior as the deflection is reduced resembles that of Series–B beams. Therefore, the E_d' value of Series–C beams can be expressed as a linear function of δ / δ_{ycal} within the deflection increasing region and by a quadratic function of δ / δ_{ycal} within the deflection decreasing region.

d) Series–D

In Fig.13 are shown some examples of load–deflection hysteresis loops for the Series–D beams. Figure 14 gives an example of the ratio of non–dimensional dissipated energy at the n–th cycle (E_d'(D(n))) for each deflection amplitude to that at the first cycle (E_d'(D(1))). Figure 15 shows the ratio of non–dimensional dissipated energy at the first cycle for each deflection amplitude of Series–D beams (E_d'(D(1))) to that of the corresponding Series–A beams at the same deflection amplitude (E_d'(A)).

Figure 14 shows that the E_d' value at a particular deflection amplitude decreases with increasing cycles of load repetition. At the deflection amplitude of 1 δ_y, the E_d' value at the second cycle has fallen to 60～80% of that at the first cycle. After ten load repetitions, the E_d' value is 40～60% of that at the first cycle. Almost the same tendency is observed at the deflection amplitude of 2 δ_y, although the reduction after ten load repetitions is somewhat smaller. When the deflection amplitude is 3 δ_y or more, on the other hand, the reduction in E_d' value is somewhat different; the fall in the E_d' value from the first cycle to the second is very small, and the total reduction ratio after ten cycles is at most 10%. At a deflection amplitude near the ultimate state, such as 6 δ_y, the E_d' value begins to decrease remarkably with repeated cycles.

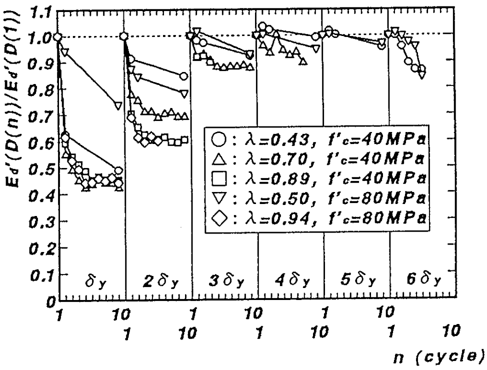

Fig.14 Changes of $E_d'(D(n))/E_d'(D(1))$ with Repeated Cycles (Series–D, $\rho_s \fallingdotseq 2.50\%$)

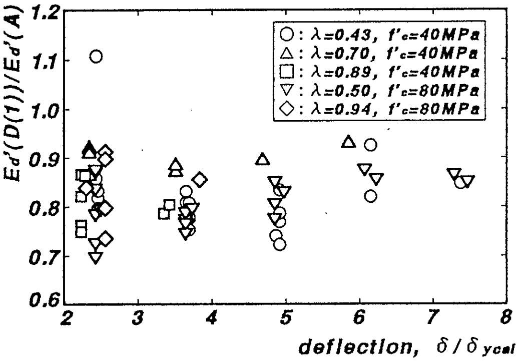

Fig.15 Relationship between $E_d'(D(1))/E_d'(A)$ and δ/δ_{ycal}

At deflection amplitudes of more than $2\delta_y$ up to the ultimate state, the E_d' value of Series–D beams after one cycle of deflection is reduced to 70~90% of that of corresponding Series–A beams at the same deflection amplitude, as seen in Fig.15. This implies that the energy dissipated at a certain deflection amplitude is influenced by the preceding number of load cycles at smaller deflection amplitudes.

These results allow the E_d' values of beams subjected to reversed cyclic loading with 10 load repetitions at each deflection amplitude to be estimated, as described below.

As mentioned previously, E_d' values at a particular deflection amplitude decrease with increasing load cycles, and the amount of the its reduction is affected by the applied deflection amplitude and the number of cycles. It can be assumed that the reduction from the first cycle to the second is the greatest, then becoming a smaller constant value from the second cycle to the tenth. It is also assumed that the E_d' values of Series–D beams at the first cycle at each deflection amplitude is lower than that of corresponding Series–A beams with only one load repetition at that amplitude. These reduction ratios are taken from the experimental data for Series–D beams.

① In the case of $\delta = \delta_y$

$$E_d'(D(1))=E_d'(A) \tag{12}$$

$$E_d'(D(n))=0.7E_d'(D(1))-\frac{0.2}{8}(n-2) \qquad (2\geqq n\geqq 10) \tag{13}$$

② In the case of $\delta = 2\delta_y$

$$E_d'(D(1))=0.83E_d'(A) \tag{14}$$

$$E_d'(D(n))=0.8E_d'(D(1))-\frac{0.1}{8}(n-2) \qquad (2\geqq n\geqq 10) \tag{15}$$

③ In the case of $\delta \geqq 3\delta_y$

$$E_d'(D(1))=0.83E_d'(A) \tag{16}$$

$$E_d'(D(n))=0.95E_d'(D(1))-\frac{0.05}{8}(n-2) \qquad (2\geqq n\geqq 10) \tag{17}$$

Where,

- $E_d'(D(1))$: non-dimensional dissipated energy at the first cycle at each deflection amplitude
- $E_d'(D(n))$: non-dimensional dissipated energy at the n-th cycle at each deflection amplitude
- $E_d'(A)$: non-dimensional dissipated energy of corresponding Series-A beam calculated from Eq.(5) at the same deflection amplitude
- n: number of cycles

Figure 16 shows a comparison of calculated E_d' values and measurements. As this shows, the calculated E_d' values coincide well with the experimental results within the range $\delta \leqq 3\delta_y$, while they tend to underestimate at deflection amplitudes of more than $4\delta_y$. This is mainly because the E_d' values at the first cycle at each deflection amplitude calculated from Eq.(14) or Eq.(16) tend to be underestimated at larger deflection amplitudes. However, the difference between measured and calculated E_d' values is relatively small and E_d' values of Series-D beams can be well estimated by this method.

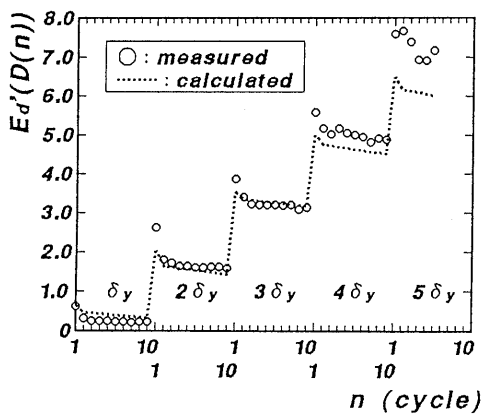

Fig.16 Example of Changes in Measured and Calculated E_d' Value (λ=0.70, ρ_s=2.66%)

3.4 Non-dimensional Total Dissipated Energy until the Ultimate State

Even if the total energy dissipated over a given loading history can be calculated as described, it is difficult to evaluate the degree of damage unless the total energy which a member can dissipate up to the ultimate state is known. Therefore, the effects of volumetric ratio of lateral confinement, mechanical degree of prestress, and loading history on the non-dimensional total dissipated energy up to the ultimate ($\Sigma E_{d\,ult.}'$) are discussed here.

Figure 17 shows the effect of loading history on the accumulation of non-dimensional dissipated energy until the ultimate state ($\Sigma E_{d\,ult.}'$). This depends on the λ-value. Where λ=0.46, the value of $\Sigma E_{d\,ult.}'$ is approximately 15% smaller under gradually decreasing cyclic loading, as Series-B tests, than that under gradually increasing loading as in Series-A. In Series-B tests, a relatively large deflection amplitude is applied at the first loading cycle. Consequently, large diagonal cracks arise during the first cycle in beams with smaller prestress, such as λ=0.46. These cracks remains open even upon unloading, resulting in a pinching of the P-δ hysteresis loop and reduced energy dissipation. On the other hand, in beams with higher λ values (λ=0.71 and 0.87), no significant difference according to loading history can be observed. In these cases, diagonal cracking is insignificant even at large deflection amplitudes and the crack restoration performance is good due to the effectiveness of higher introduced prestress. From these results, the effect of loading history on the accumulation of dissipated energy in partially prestressed concrete beams is shown to become smaller with increasing λ value.

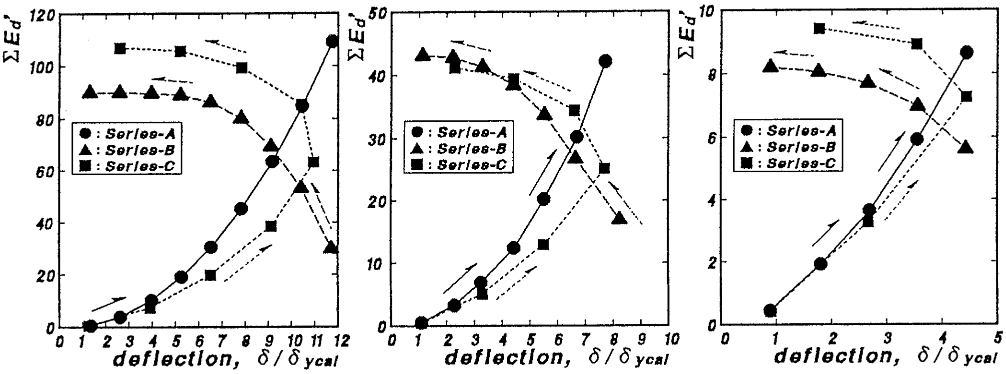

(a) λ =0.46 (b) λ =0.71 (c) λ =0.87

Fig.17 Effects of Loading Histories on $\Sigma E_d'$ (ρ_s=2.43%)

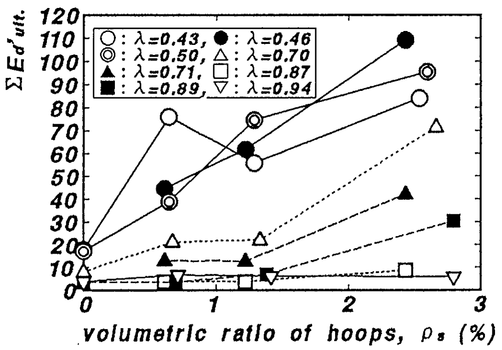

Fig.18 Effects of ρ_s on $\Sigma E_{d}'{}_{ult.}$ Value (Series–A)

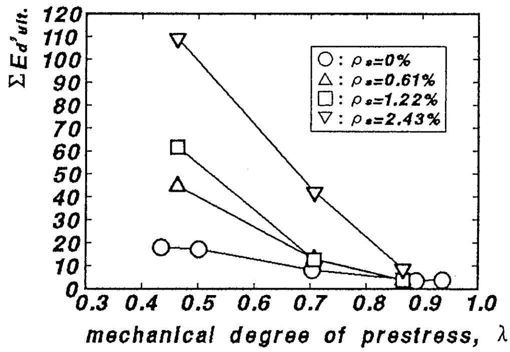

Fig.19 Effects of λ on $\Sigma E_{d}'{}_{ult.}$ Value (Series–A)

In Fig.18 and Fig.19, the effects of volumetric ratio of lateral confinement (ρ_s) and mechanical degree of prestress (λ) on non–dimensional total dissipated energy until the ultimate state ($\Sigma E_{d}'{}_{ult.}$) are shown for Series–A beams. The $\Sigma E_{d}'{}_{ult.}$ value increases with increasing ρ_s within the range $0 \leqq \rho_s \leqq 2.80\%$, and a quadratic relation between $\Sigma E_{d}'{}_{ult.}$ and ρ_s can be assumed under constant λ value. On the other hand, the value of $\Sigma E_{d}'{}_{ult.}$ decreases with increasing λ value within the range $0.43 \leqq \lambda \leqq 0.94$ and can be assumed to be almost inversely proportional to λ when ρ_s is constant. Further, the effectiveness of lateral confinement on improvement to the energy dissipation properties is dependent of λ . From these results, the $\Sigma E_{d}'{}_{ult.}$ value can be expressed as in Eq.(18).

$$\Sigma E'_{d_{ult.}} = a\,\rho_s^{\,2} + b\left(\frac{1}{\lambda}\right) + c\left(\frac{\rho_s^{\,2}}{\lambda}\right) + d \tag{18}$$

The values of the coefficients, a, b, c, and d should be estimated separately for Series–A beams and Series–D beams, since $\Sigma E_{d}'{}_{ult.}$ values of Series–D beams are substantially higher than those of Series–A beams as a result of ten load repetitions at each deflection amplitude. On the other hand, the values of these coefficients estimated for Series–A beams should be applicable to Series–B and Series–C beams since the total dissipated energy up until the ultimate state is not very different among the three series, although the $\Sigma E_{d}'{}_{ult.}$ values of Series–B beams are somewhat smaller.

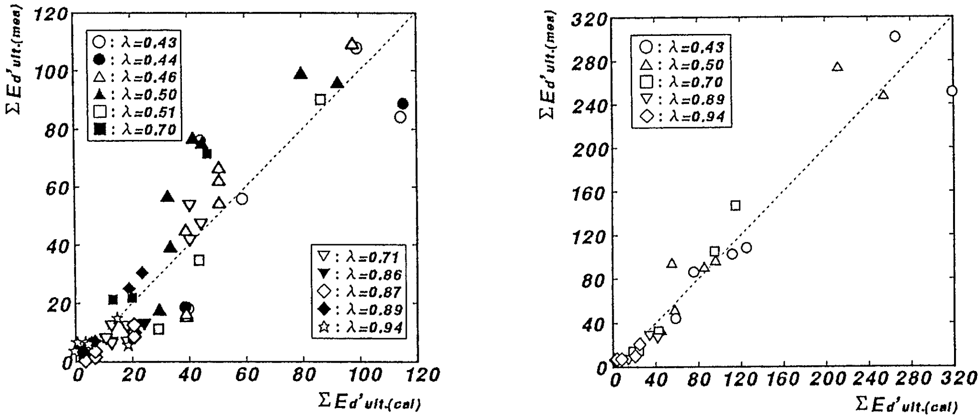

(a) Series–A (b) Series–D

Fig.20 Comparison between $\Sigma E_d'{}_{ult.(mea)}$ Values and $\Sigma E_d'{}_{ult.(cal)}$ Values

The coefficients a, b, c, and d obtained for Series–A beams by regression analysis of the test results are as follows:

a=–5.52, b=32.48, c=7.44, d=–35.20 (standard deviation of $\Sigma E_d'{}_{ult.}$ is 13.52)

On the other hand, the values of these coefficients for Series–D beams are the following:

a=–29.39, b=45.69, c=30.28, d=–46.44 (standard deviation of $\Sigma E_d'{}_{ult.}$ is 24.01)

Each calculated value of the non–dimensional total dissipated energy until the ultimate state obtained from Eq.(18) ($\Sigma E_d'{}_{ult.(cal)}$) is indicated together with the measured value ($\Sigma E_d'{}_{ult.(mea)}$) in Figs.20–(a) and (b) for Series–A and Series–D beams, respectively. These figures show that $\Sigma E_d'{}_{ult.}$ values can be estimated to a certain degree, although the discrepancy between measured and calculated $\Sigma E_d'{}_{ult.}$ is relatively large in Series–A beams, as indicated by the standard deviation of 13.52. This is mainly because only the effects of volumetric ratio of lateral confinement and mechanical degree of prestress are considered in the calculation process

3.5 Damage Evaluation Based on Hysteretic Dissipated Energy

If the degree of seismic damage to concrete structures or members under earthquake loading could be expressed numerically, it would be a criterion by which to carry out repairs or strengthening to damaged structures. Here we discuss the possibility of evaluating seismic damage based on hysteretic dissipated energy.

A damage index (DI) as Eq.(19) in this study is defined.

$$DI=\frac{\Sigma E_d'}{\Sigma E_{d_{ult.}}'} \tag{19}$$

Where,

$\Sigma E_d'{}_{ult.}$: the non–dimensional total energy which can be dissipated by a member until the ultimate state for a given loading history

$\Sigma E_d'$: the actual accumulated non–dimensional energy dissipated during loading

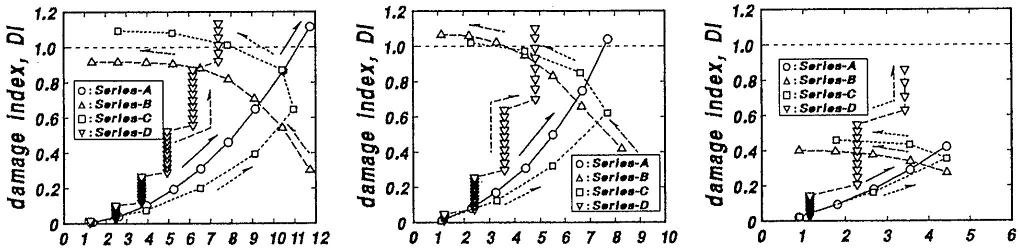

(a) $\lambda \fallingdotseq 0.46$ (b) $\lambda \fallingdotseq 0.71$ (c) $\lambda \fallingdotseq 0.87$

Fig.21 Examples of Changes in DI ($\rho_s \fallingdotseq 2.50\%$)

DI=0 represents the no damage situation and DI=1.0 means that a member has reached its ultimate state; that is, in this study, when the load carrying capacity at a given deflection amplitude falls to 80% of the maximum ultimate load.

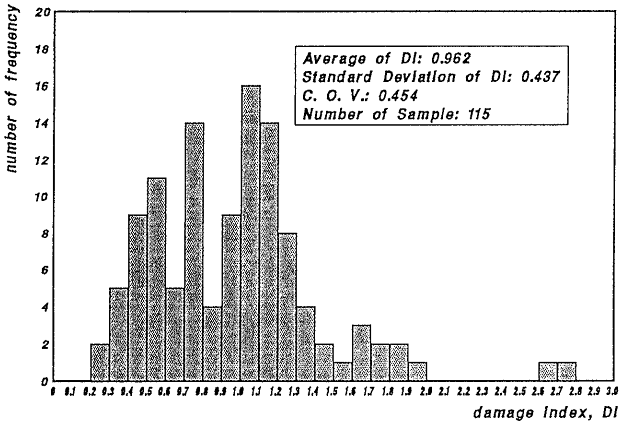

Fig.22 Statistics of DI in the Ultimate State

As mentioned previously, the value of $\Sigma E_d'_{ult.}$ differs with the number of repeated cycles at a particular deflection amplitude. This implies that the effect of dissipated energy after the second cycle on the degree of damage is different from that of the first loading at the same deflection amplitude. In consideration of practical application, therefore, it is desirable to modify the $\Sigma E_d'$ value where several load repetitions take place at the same deflection amplitude by using a reduction factor which considers the effect of dissipated energy on the amount of real damage. The damage can then be evaluated using the modified $\Sigma E_d'$ value and the $\Sigma E_d'_{ult.}$ value for a basic loading history which is already known, for example, Series–A. In this paper, however, DI values of Series–D beams are calculated from the $\Sigma E_d'$ values without modification and the $\Sigma E_d'_{ult.}$ values are calculated from Eq.(18) using the coefficients for Series–D beams. As for the Series–B and Series–C beams, on the other hand, $\Sigma E_d'_{ult.}$ values are calculated using the coefficients for Series–A beams.

Figure 21 shows some examples of the changes in DI during loading tests. In Series–A, the degree of damage is small at an early stage of loading and the ratio of accumulated damage rises with increasing applied deflection amplitude. In Series–B, on the other hand, the DI value after the first cycle reaches 0.3~0.4. This implies that the beams are significantly damaged if subjected to a deflection close to the ultimate value at the first cycle of loading. Subsequently, however, the increase in accumulated damage becomes smaller. In Series–D beams, damage is accumulated as ten load repetitions take place at each deflection amplitude, and the ultimate state is reached at a smaller deflection amplitude as compared with the corresponding Series–A beam. In case of the beams with λ =0.87, the DI value does not reach 1.0 even at the end of loading. This is mainly because the relative difference between calculated $\Sigma E_d'_{ult.}$ and the actual value is large since the $\Sigma E_d'_{ult.}$ value itself is smaller than that of a beam with a lower λ value.

In Fig.22, a histogram of DI corresponding to the ultimate state calculated for each beam is shown. A high degree of scatter (C.O.V.=0.454) in the DI value at the ultimate state is observed, although the average value of DI is almost 1.0. The relative difference tends to be particularly large in the case of beams with higher λ value and lower ρ_s value. This is mainly due to the greater uncertainty in the definition of the ultimate state under reversed cyclic loading and in the effects of test variables.

As previously mentioned, non–dimensional total dissipated energy up until the ultimate state is affected by not only the test variables adopted in this study but also by certain other factors. Therefore, further investigations of energy dissipation properties are necessary in order to establish an evaluation method for seismic damage to concrete structures based on hysteretic dissipated energy.

4. CONCLUSIONS

In this paper, the effects of various test variables on the energy dissipation properties of partially prestressed concrete beams are investigated. In addition, a damage index based on hysteretic dissipated energy is proposed based on the experimental results. The main conclusions reached in this work are as follows.

(1) The energy dissipation properties of partially prestressed concrete beams are affected mainly by volumetric ratio of lateral confinement and mechanical degree of prestress. The effects of concrete compressive strength, longitudinal steel index, and shear span–effective depth ratio are relatively small in comparison.

(2) The non–dimensional dissipated energy, which is the dissipated energy normalized by the product of calculated yield load and yield deflection, of partially prestressed concrete beams is also influenced by the loading history. The value of non–dimensional dissipated energy at each deflection amplitude can be expressed as a linear function of the applied deflection amplitude as the deflection increases, and as a quadratic as the deflection decreases. The values of the coefficients in these functions depend mainly on the level of mechanical degree of prestress.

(3) The non–dimensional dissipated energy at a particular deflection amplitude decreases with increasing cycles. The rate of decrease is affected by the applied deflection amplitude and the number of cycles. The non–dimensional dissipated energy at the first of ten load repetitions is less than where only one repetition takes place at each deflection amplitude.

(4) The non–dimensional total dissipated energy up until the ultimate state increases with increasing volumetric ratio of lateral confinement, while it decreases with increasing mechanical degree of prestress. It can be estimated to a certain extent by a function of these two variables. The value of non–dimensional total dissipated energy until the ultimate state is almost constant if the sum of applied deflection amplitudes is the same, although it tends to be somewhat smaller with less mechanical degree of prestress where the deflection is gradually decreased , as in Series–B.

(5) The degree of damage to partially prestressed concrete beams under reversed cyclic loading can be expressed quantitatively by a damage index based on the hysteretic dissipated energy. However, further investigations on the process of dissipated energy accumulation are necessary for a more accurate evaluation of seismic damage to concrete structures.

References

[1] Public Works Research Center: Manual for Restoration of Civil Engineering Structures Damaged during Earthquakes, Ministry of Construction, 1986

[2] Park, Y. J. and Ang, A. H–S.: Mechanistic Seismic Damage Model for Reinforced Concrete, Journal of Structural Engineering, ASCE, Vol.111, No.4, pp.722–739, 1985

[3] Uomoto, T., Yajima, T., and Hongo, K.: Damage Evaluation of Reinforced Concrete Beams Subjected to Cyclic Bending Moment Using Dissipated Energy, Proc. of JSCE, No.460/V–18, pp.85–92, 1993

[4] Stephens, J. E. and Yao, J. T. P.: Damage Assessment Using Response Measurements, Journal of Structural Engineering, ASCE, Vol.113, No.4, pp.787–801, 1987

[5] Kobayashi, K., Inoue, S., and Matsumoto, T.: Inelastic Behavior of Partially Prestressed Concrete under Reversed Cyclic Loading, Proc. of the 5th Canadian Conference on Earthquake Engineering, Ottawa, pp.841–848, 1987

[6] Inoue, S., Kobayashi, K., and Katsuno, Y.: Inelastic Deformation Properties of Partially Prestressed Concrete Beams under Reversed Cyclic Loading, Proc. of the 42nd Annual Conference of the JSCE, Vol.5, pp.232–233, 1987

[7] Igo, Y. et al.: Load Carrying Capacity of Partially Prestressed Concrete Members under Reversed Cyclic Loading, Proc. of the 43rd Annual Conference of the JSCE, Vol.5, pp.610–611, 1988

[8] Inoue, S. et al.: Application of Rectangular Hoop as Lateral Confinement for Concrete Beam Members, CAJ Proceedings of Cement & Concrete, No.43, pp.340–345, 1989

[9] Inoue, S. et al.: Effect of Loading Histories on the Energy Dissipation of Partially Prestressed Concrete Beams and Their Damage Evaluation, Proc. of the JCI, Vol.15, No.2, pp.401–406, 1993

[10] Fukushima, Y. et al.: Effects of Various Factors on the Dissipated Energy of Partially Prestressed Concrete Beams, Proc. of Annual Meeting of the JSCE Kansai Branch, pp.V–5–1–V–5–2, 1993